



International Journal of

ROBOTICS & AUTOMATION

VOLUME 23, Number 1, 2008

• Dynamic Modelling for Cooperation System of Flexible Robots Manipulating a Constrained Object	<i>Y.-Q. Yu, C.-X. Zhang</i>	1
• Face Alignment based on Statistical Models and Gabor Wavelets	<i>M.-S. Yu, S.-F. Li</i>	9
• An Automatic Bi-Channel Compression Technique for Medical Images	<i>M.A.-R. Abdou, M.B. Tayel</i>	15
• Resolve Redundancy with Constraints for Obstacle and Singularity Avoidance Subgoals	<i>C. Qiu, Q. Cao, Y. Sun</i>	22
• Feedforward Control of Flexible Link Systems using Parallel Solution Scheme	<i>D. Isobe, A. Kato</i>	31
• Strategic Functions for Feedback Stabilization of Bilinear Systems	<i>M. Ouzahra, R. El Ayadi</i>	40
• Target Tracking Robotic Manipulation Theories Applied to Force/Position Control in Peg-in-Hole Assembly Tasks	<i>D.J. Giblin, Y. Liu, K. Kazerounian</i>	49
• Development of a Precision Parallel Micro-Mechanism for Nano Tele-Operation	<i>J. Wang, S. Guo</i>	56
Information for Submission of Papers to Journals		64
Upcoming Conference List		66

DEVELOPMENT OF A PRECISION PARALLEL MICRO-MECHANISM FOR NANO TELE-OPERATION

J. Wang* and S. Guo**

Abstract

There is an urgent need for nano-level teleoperation systems to carry out three-dimensional high-speed micromanipulations for medical and biotechnological applications. The authors have designed a precision parallel micro-mechanism driven by piezo actuators (PZT) for use as an operating robot with six degrees of freedom, maximum movement of 18 to 28 μm , and a resolution of 8 to 25 nm. Here, they present the conceptual design, synthesis, and control strategy along with an evaluation of the precision parallel micro-mechanism of this system. The experimental results indicate that the developed parallel micro-mechanism can be used to manipulate micro-objects at high speed and with a high degree of precision.

Key Words

Micro-operation, biotechnology, micro-mechanism, piezo actuator, parallel robot

1. Introduction

Recently, there has been a great deal of progress in the biosciences due to advances in biotechnology, such as genetic engineering, cell engineering, and developmental engineering [1-5]. Research in these fields requires micro- and nano-manipulations, mass production, and repetitive, high-speed, high-precision processing. Consequently, human-scale nano-teleoperation systems have been developed [6, 7]. Numerous potential applications are unsuitable for conventional robotics due to the size of the objects to be manipulated [8]. When the manipulated object is extremely small, such as a cell or an embryo, the manipulation system must consist of fine macro- and micro-scale mechanisms, and make use of a complex fine motion control system. Physical phenomena at the micro-scale

differ from those at the macro-scale. Therefore, such manipulation systems must be designed carefully. The key technologies include manipulators, micro-systems, visualization systems, human interfaces, and automation technologies. New approaches must be developed to address the challenge of high-speed micromanipulation.

Most industrial manipulators have serial open-ended structures. The human arm is a good example of a serial manipulator. A parallel manipulator is a closed-loop mechanism, with higher speed, stiffness, and payload capacity as well as better accuracy than serial manipulators. Therefore, we used a parallel structure to develop our micromanipulator.

Many types of micro-operation system have been developed. One type was designed for working with large objects over mini- or micro-scale distances, driven by lead zirconate titanate (PZT) actuators, shape memory alloys (SMA), or magnetic actuators. Another type was designed for working with miniature objects driven using high-speed electrostatic actuators or SMA thin-film micro-actuators. After comparing the various actuators currently available, we determined that a PZT actuator was the best fit for our design because of its small workspace, high rigidity, and high speed.

Therefore, we designed a precision parallel micro-mechanism driven by PZT actuators for use as an operating robot with six degrees of freedom (DOF), maximum movement of 18 to 28 μm , and a resolution of 8 to 25 nm for human-scale teleoperation systems. Here, we present the conceptual design, synthesis, and control strategy of this system, and evaluate the precision parallel micro-mechanism in the following sections.

2. Conceptual Design for the Parallel Micro-mechanism

In the conceptual design stage, a "best" conceptual design was selected from several alternatives. A 3-3 octahedral structure was first considered, as it is the simplest structure of its kind. We used this structure on the top platform. The mobility of general spatial mechanisms can be calculated from Grubler's criterion [9]:

* Graduate School of Engineering, Kagawa University, 2217-20 Hayashi-cho, Takamatsu, Kagawa, Japan; email: s05d502@stmail.eng.kagawa-u.ac.jp

** Faculty of Engineering, Kagawa University, 2217-20 Hayashi-cho, Takamatsu, Kagawa, Japan, and Harbin Engineering University, 145 Nantong Street, Harbin, Heilongjiang, China; email: guo@eng.kagawa-u.ac.jp

Recommended by Dr. Jingzhou Yang
(paper no. 206-3141)

$$M = \lambda(n - 1) - \sum_{i=1}^i (\lambda - f_i) \quad (1)$$

where:

- M : Mobility, or number of degree of freedom of the system
- λ : Degrees of freedom of the space in which a mechanism is intended to function, for the spatial case, $\lambda = 6$
- n : Numbers of linkages in the mechanism, including the fixed linkages
- i : Numbers of joints in a mechanism, assuming that all the joints are binary
- f_i : Degrees of relative motion permitted by joint i

As shown in Fig. 1, our parallel platform had a total of 14 bodies: the top platform, the base platform, and two bodies for each of the six legs. If we used spherical joints to connect the linkages, each spherical joint had three degrees of relative freedom, and thus there were a total of 12 joints, each of which had three degrees of relative freedom. Thus, the mobility equation is:

$$M = 6(14 - 1) - \sum_{i=1}^{12} (6 - 3) - \sum_{i=1}^6 (6 - 1) = 12 \quad (2)$$

To eliminate the six additional rotational freedoms due to the spherical joints, these were replaced by six elastic wire joints connecting the upper platform and the leg connectors [10]. When an elastic wire is bent, its rotation centre deviates from its original position, introducing an accuracy problem in the elastic element. Therefore, our elastic wires were designed with sufficient hardness to prevent any movement of the rotation centre so that the accuracy problem caused by bending could be neglected. This type of elastic wire joint has been used in several successful mechanisms, such as the "two-fingered micro-hand" developed by Arai [11]. We then calculated the mobility of the 6-6 parallel platform from:

$$M = 6(14 - 1) - \sum_{i=1}^6 (6 - 3) - \sum_{i=1}^6 (6 - 2) - \sum_{i=1}^6 (6 - 1) = 6 \quad (3)$$

The parallel mechanism had six degrees of freedom. As the precise dimensions of the object to be manipulated were uncertain, the movement range and resolution of the precision micro-mechanism were designed to be adjustable. We wished to design a mechanism capable of manipulating micro-objects ranging in size from 5×10^{-9} to 7×10^{-5} m with an adjustable resolution of less than 20 nm. This differed from other research projects reported to date [12-15].

The proposed precision parallel mechanism is shown in Fig. 1. It consisted of four parts, the first of which was the upper platform to which the moving part of the operating hand was fixed. The second part consisted of six linkages. Due to the small workspace and high resolution, there were two elastic wire joints at both ends of each linkage. Each

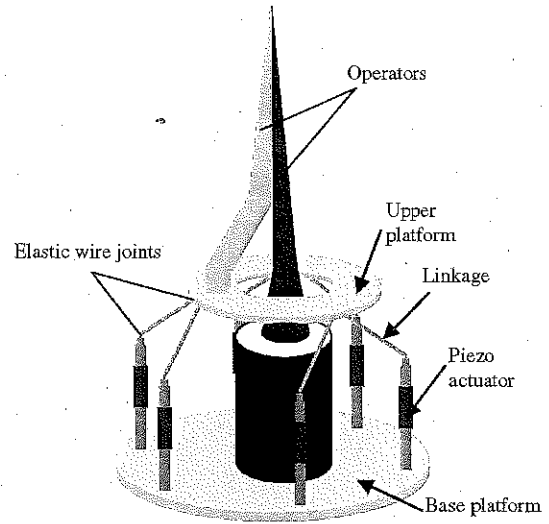


Figure 1. The proposed parallel micro-mechanism.

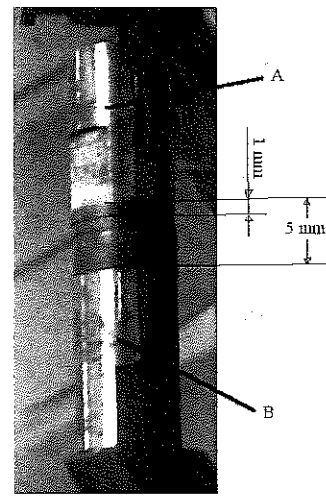


Figure 2. The length-adjustable linkages.

linkage included five spacers with a height of $1.0 \pm 0.1 \mu\text{m}$. As shown in Fig. 2, the length of the linkages could be adjusted from 33.22 to 38.22 mm in 1-mm steps. We designed the linkages as screws so that the clearance could be varied. To adjust the lengths of the linkages, spacers can be simply removed or inserted and then Part A (bolt) and Part B (nut) are fastened together tightly. The third part consisted of six PZT actuator containers designed to grow by a given displacement in only one direction as the actuator is extended. The fourth part was the base platform. The PZT actuator containers were fixed on the base platform in a circle (C) the radius of which could be adjusted from 29 to 43 mm in 2-mm steps, as shown in Fig. 3, with an allowable error of $\pm 0.1 \mu\text{m}$. We placed six screw holes (S) in the side of the base platform to avoid the clearance of the adjustable radius of the base platform. To adjust the radius of the base platform, bolts of constant length were used for individual adjustment of each of the six sides.

The operating hands had two parts: one fixed to the upper platform and the other fixed to the base platform.

We could adjust the length of the linkages and radius of the base platform to perform the operations required for different types of work. Elastic wire joints were used to maintain the high degree of accuracy.

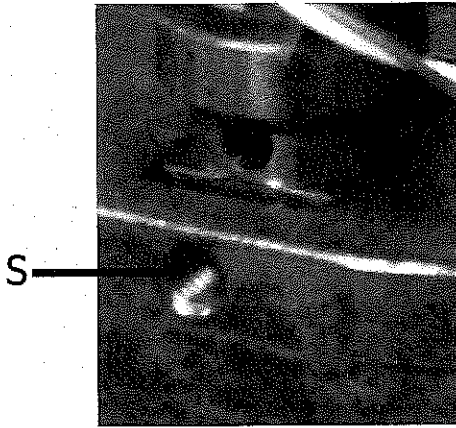


Figure 3. The diameter-adjustable base platform.

3. Synthesis of the Parallel Micro-mechanism

A model of the parallel micro-mechanism is shown in Fig. 4. In the model, we set a fixed O-XYZ coordinate system at point O and a moving $o'-x'y'z'$ coordinate system at point o' . Therefore, the absolute coordinates of point o' are $(0, 0, h + \sqrt{L^2 - (R-r)^2})$, where L is the length of the linkage, r is the radius of the upper platform, R is the radius of the base platform, and h is the height of the PZT actuator container. As a result, we obtain:

$$S = \sqrt{(R \cos |\theta_i - \xi_i| - r)^2 + (R \sin |\theta_i - \xi_i|)^2} \quad (4)$$

where θ_i is the angle between each joint of the upper platform and axis X. ξ_i is the angle between each joint of the base platform and axis X, ξ_i is set to $i \times 60^\circ$, and S is the displacement between each joint of the base platform and the projection of each joint of the top platform on the base platform.

In the moving coordinate system, the coordinates of each joint point of the upper platform are defined as

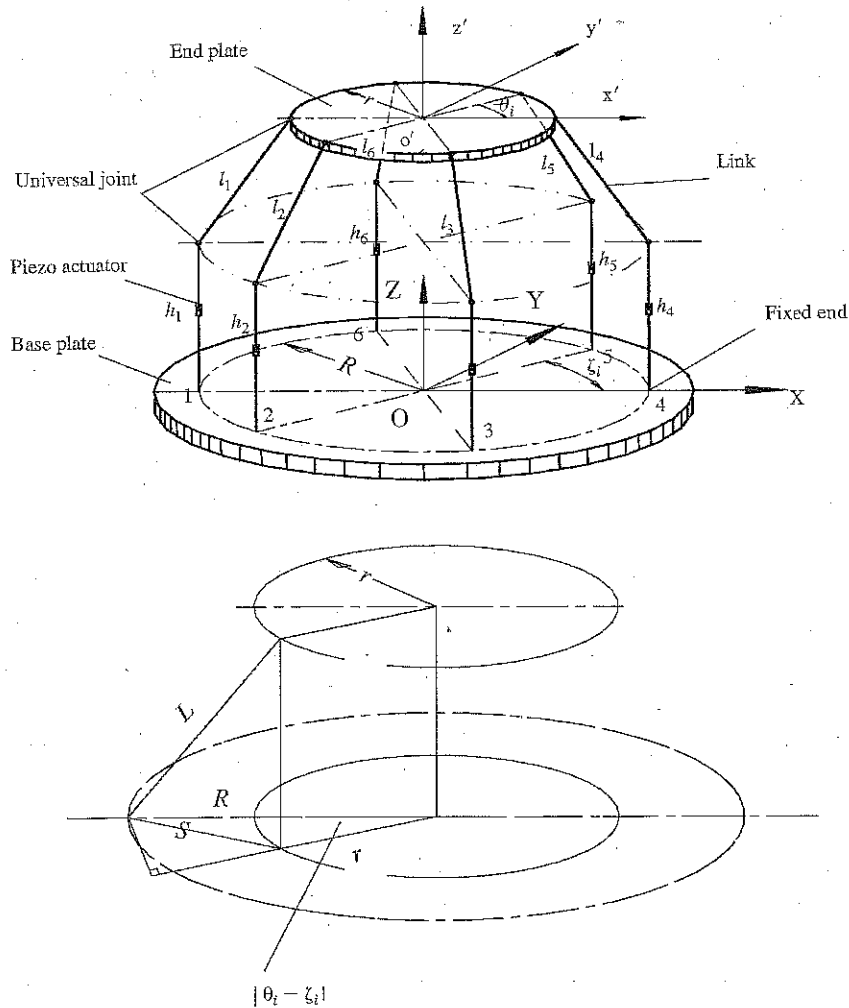


Figure 4. The model of the parallel micromechanism.

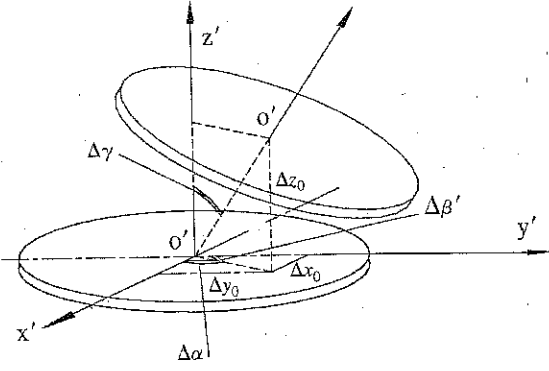


Figure 5. The movement of the upper platform.

$(x_i, y_i, 0)$, where $x_i = r \cos \theta_i$, $y_i = r \sin \theta_i$. Assuming that the movement of the origin of the moving coordinate system is $(\Delta x_0, \Delta y_0, \Delta z_0, \Delta \alpha, \Delta \beta, \Delta \gamma)$, $\Delta \alpha$ is the angle between $o'x'$ and the projection of the normal of the moved top platform on the fixed top platform, $\Delta \beta$ is the angle between $o'y'$ and the projection of the normal of the moved top platform on the fixed top platform, and $\Delta \gamma$ is the angle between $o'z'$ and the normal of the moved top platform. As shown in Fig. 5, the movement of each joint of the upper platform is given by:

$$\begin{cases} \Delta x_i = \Delta x_0 - y_i \cdot \Delta \gamma + z_i \cdot \Delta \beta \\ \Delta y_i = \Delta y_0 - x_i \cdot \Delta \gamma + z_i \cdot \Delta \alpha \\ \Delta z_i = \Delta z_0 - x_i \cdot \Delta \beta + y_i \cdot \Delta \alpha \end{cases} \quad (5)$$

The absolute coordinates of each point on upper platform are given by:

$$\begin{cases} x'_i = x_0 + r \cos \theta_i + \Delta x_0 - y_i \cdot \Delta \gamma + z_i \cdot \Delta \beta \\ y'_i = y_0 + r \sin \theta_i + \Delta y_0 + x_i \cdot \Delta \gamma - z_i \cdot \Delta \alpha \\ z'_i = z_0 + 0 + \Delta z_0 - x_i \cdot \Delta \beta + y_i \cdot \Delta \alpha \end{cases} \quad (6)$$

where $x_0 = y_0 = 0$ and $z_0 = h + \sqrt{L^2 - (R-r)^2}$.

Differentiating each side of (6), the next equation can be obtained:

$$\begin{cases} dx'_i = dx_0 - y_i \cdot d\gamma \\ dy'_i = dy_0 + x_i \cdot d\gamma \\ dz'_i = dz_0 - x_i \cdot d\beta + y_i \cdot d\alpha \end{cases} \quad (7)$$

Then, (8) can be obtained as:

$$L^2 = (x'_i - X_i)^2 + (y'_i - Y_i)^2 + (z'_i - Z_i)^2 \quad (8)$$

where $X_i = R \cos \xi_i$, $Y_i = R \sin \xi_i$, $Z_i = h_i$.

Differentiating each side of (8), we obtain the following with (4):

$$\begin{aligned} & (r \cos \theta_i - R \cos \xi_i)(dx_0 - r \sin \theta_i \cdot d\gamma) + (r \sin \theta_i - R \sin \xi_i) \\ & \times (dy_0 + r \cos \theta_i \cdot d\gamma) + 2\sqrt{L^2 - (R-r)^2} \\ & \times (dz_0 - r \cos \theta_i \cdot d\beta + r \sin \theta_i \cdot d\alpha - dh_i) = 0 \end{aligned} \quad (9)$$

Suppose that:

$$\begin{cases} A_i = r \cos \theta_i - R \cos \xi_i \\ B_i = r \sin \theta_i - R \sin \xi_i \\ rs_i = r \sin \theta_i \\ rc_i = r \cos \theta_i \\ M = \sqrt{L^2 - (R-r)^2} \end{cases} \quad (10)$$

Finally, (11) is obtained as follows:

$$M \begin{bmatrix} dh_1 \\ dh_2 \\ dh_3 \\ dh_4 \\ dh_5 \\ dh_6 \end{bmatrix} = \begin{bmatrix} A_1 & B_1 & M & M \cdot rs_1 & -M \cdot rc_1 & B_1 \cdot rc_1 & -A_1 \cdot rs_1 \\ A_2 & B_2 & M & M \cdot rs_2 & -M \cdot rc_2 & B_2 \cdot rc_2 & -A_2 \cdot rs_2 \\ A_3 & B_3 & M & M \cdot rs_3 & -M \cdot rc_3 & B_3 \cdot rc_3 & -A_3 \cdot rs_3 \\ A_4 & B_4 & M & M \cdot rs_4 & -M \cdot rc_4 & B_4 \cdot rc_4 & -A_4 \cdot rs_4 \\ A_5 & B_5 & M & M \cdot rs_5 & -M \cdot rc_5 & B_5 \cdot rc_5 & -A_5 \cdot rs_5 \\ A_6 & B_6 & M & M \cdot rs_6 & -M \cdot rc_6 & B_6 \cdot rc_6 & -A_6 \cdot rs_6 \end{bmatrix} \times \begin{bmatrix} dx_0 \\ dy_0 \\ dz_0 \\ d\alpha \\ d\beta \\ d\gamma \end{bmatrix} \quad (11)$$

Here, we define matrix P as:

$$P = \begin{bmatrix} A_1 & B_1 & M & M \cdot rs_1 & -M \cdot rc_1 & B_1 \cdot rc_1 & -A_1 \cdot rs_1 \\ A_2 & B_2 & M & M \cdot rs_2 & -M \cdot rc_2 & B_2 \cdot rc_2 & -A_2 \cdot rs_2 \\ A_3 & B_3 & M & M \cdot rs_3 & -M \cdot rc_3 & B_3 \cdot rc_3 & -A_3 \cdot rs_3 \\ A_4 & B_4 & M & M \cdot rs_4 & -M \cdot rc_4 & B_4 \cdot rc_4 & -A_4 \cdot rs_4 \\ A_5 & B_5 & M & M \cdot rs_5 & -M \cdot rc_5 & B_5 \cdot rc_5 & -A_5 \cdot rs_5 \\ A_6 & B_6 & M & M \cdot rs_6 & -M \cdot rc_6 & B_6 \cdot rc_6 & -A_6 \cdot rs_6 \end{bmatrix} \quad (12)$$

If $|P| = 0$, there will be a singularity point; however, we used elastic wire joints to allow us to ignore the singularity points while maintaining the system accuracy.

Fig. 6 shows a photograph of developed parallel micro-mechanism prototype. The specifications and product parameters measured using a laser interferometer are listed in Table 1. We used a 12-bit DC PCI-3341A board to control the PZT actuators, to obtain the desired resolution as described by:

$$\delta \approx \frac{1}{6} \sum_{i=1}^6 2^{-12} \frac{\Delta h_{\max} L}{(R-r) \cos |\theta_i - \xi_i|} \quad (13)$$

where Δh_{\max} is the maximum displacement of the PZT actuator. The calculated example results are shown in Fig. 7.

If we suppose that the maximum displacement of the PZT actuators is $17.4 \mu\text{m}$, we can use (11) and the product parameters to calculate the workspace for the parallel micro-mechanism by adjusting L and R . Two example results are given in Table 2.

4. Control Strategy for the Parallel Micro-mechanism

Our control strategy is shown in Fig. 8. We aimed to design a parallel micro-mechanism for both micro- and nano-scale operations, so high stiffness and a high degree of accuracy were required with no voice or shock. Based on these requirements and the desired dimensions, we selected a piezo-electric multilayer actuator (AE0505D16) with a

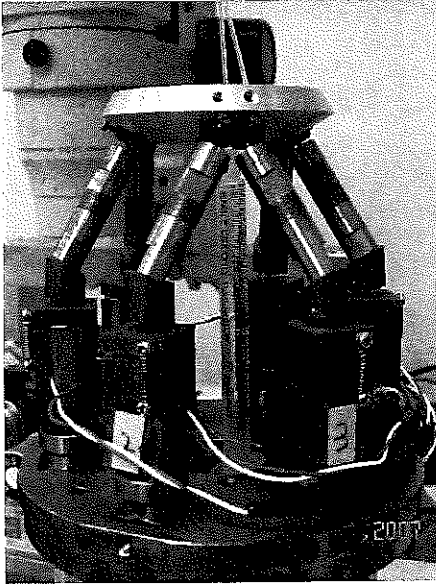


Figure 6. The manufactured parallel micro-mechanism.

maximum displacement of $17.4 \mu\text{m}$ to drive the parallel micro-mechanism.

We used a foil strain-gauge (force feedback system) to test the performance for this type of actuator by changing the control voltage from 0 to 150 V in 2-V and 0.5-s steps. The test results are shown in Fig. 9. There was some hysteresis in the actuators, but the relationship was reasonably linear, which allowed them to be used in our micro-mechanism.

A good actuator driver was also required. We selected the ENP-150U actuator driver made by Echo Electronics for our research. This type of driver shows high performance and can be easily controlled remotely.

We developed the control software using VC++, as shown in Fig. 10.

5. Evaluating the Precision Parallel Micro-mechanism

In these tests, we set $R=43 \text{ mm}$ and $L=38.22 \text{ mm}$ as default values. The other parameters were set as listed in Table 1.

The parallel micro-mechanism was a closed structure that used elastic wire joints, making the method of movement very complex. Therefore, we drove the PZT actuators in groups. We numbered the actuators from 1 to 6, and placed them in three groups based on a 3-3 octahedral structure [9]: Nos. 1 and 6 were in Group 1, Nos. 2 and 3 were in Group 2, and Nos. 4 and 5 were Group 3. We

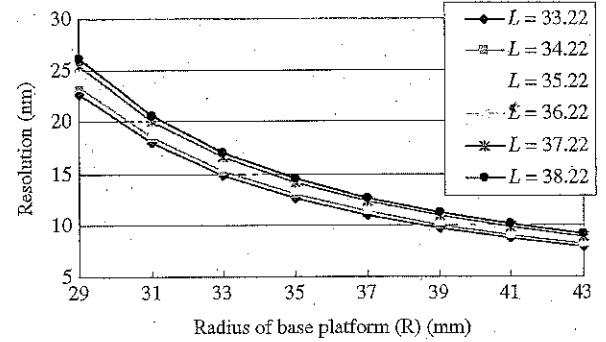


Figure 7. The relationships between resolution and changeable parameters (R is the radius of the base platform, L is the length of the linkages).

Table 1

The Specifications and Product Parameters of the Manufactured Parallel Micro-mechanism

Size	112 mm (L) × 112 mm (W) × 102 mm (H)
Radius of the Base Platform (R)	29 ~ 43 mm
Radius of the Upper Platform (r)	21.5 mm
Length of the Linkages (L)	33.22 ~ 38.22 mm
$\theta_i (i=1 \sim 6)$	$0^\circ, 105^\circ, 120^\circ, 225^\circ, 240^\circ, 345^\circ$
$\xi_i (i=1 \sim 6)$	$0^\circ, 60^\circ, 120^\circ, 180^\circ, 240^\circ, 300^\circ$

Table 2
The Example Results for the Workspace and Resolution.

Parameter	$L = 33.22 \text{ mm}, R = 43 \text{ mm}$	$L = 38.22 \text{ mm}, R = 29 \text{ mm}$
Approximate workspace(xyz)	$11.8 \times 11.8 \times 18.4 \mu\text{m}$	$28.4 \times 28.4 \times 28.2 \mu\text{m}$
Resolution	10 nm less	10 nm more

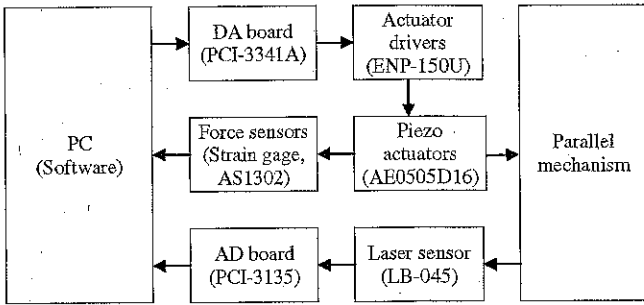


Figure 8. The control strategy for the parallel micro-mechanism.

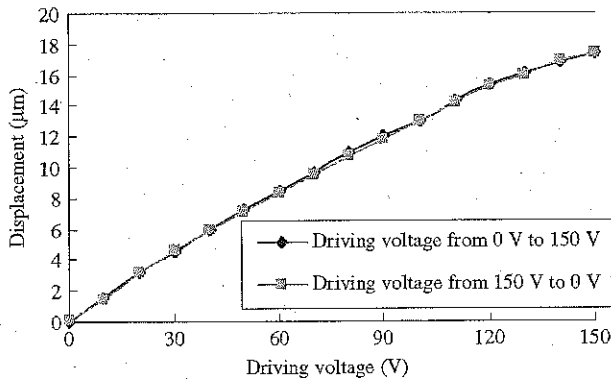


Figure 9. The relationships between displacement and applied voltage for the selected PZT actuator with force feedback system.

could drive all of the PZT actuators individually, or with three voltages in the tests to determine the movement of the centre of the upper platform.

The following three tests were conducted.

1. *Controlling all the actuators using the same input voltage.* In this case, we controlled all three groups of actuators using the same input voltages, ranging from 0 to 150 V in 0.75-V and 0.1-s steps. The results are shown in Fig. 11.
2. *Controlling the actuators group by group.* In this test, we drove the actuators in each group separately, starting with Group 1 and ending with Group 3. The driving voltage of each group ranged from 0 to 150 V in 0.75-V and 0.1-s steps. The results are shown in Fig. 12.
3. *Controlling the actuators individually.* We also drove the actuators individually, in numerical order starting with No. 1 and ending with No. 6. The driving voltage of each actuator ranged from 0 to 150 V in 0.75-V and 0.1-s steps. The results are shown in Fig. 13.

Based on the results of these three tests, we determined that the proposed parallel micro-mechanism could be controlled at high speed using the six Piezo actuators, and that the designed working range could be achieved.

To avoid hysteresis, we plan to control the parallel micro-mechanism with a closed loop using a force feedback system, such as foil strain-gauge sensors.

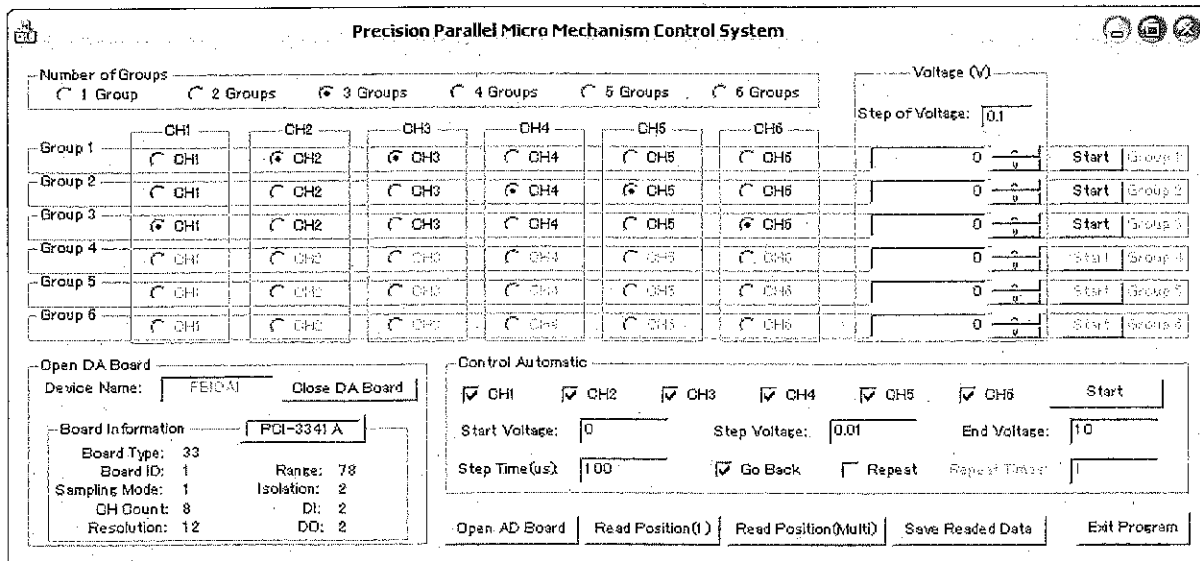


Figure 10. Control software for developed parallel micro-mechanism.

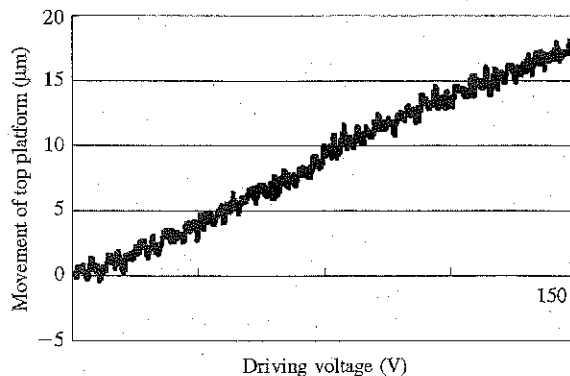


Figure 11. Test 1: Controlling all the actuators using the same input voltage.

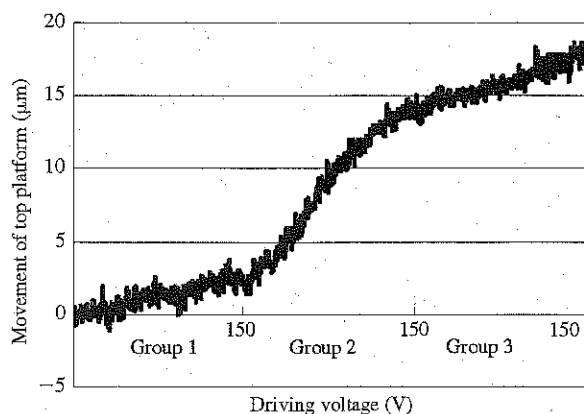


Figure 12. Test 2: Controlling the actuators group by group.

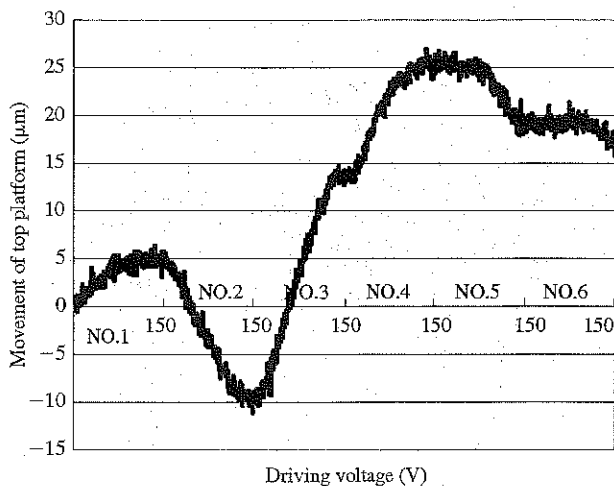


Figure 13. Test 3: Controlling the actuators individually.

6. Conclusion

We have designed a six-DOF precision parallel micro-mechanism driven by PZT actuators with a maximum movement of 18 to 28 μm and a resolution of 8 to 25 nm for nano teleoperation applications. We presented a

conceptual design to illustrate how our micro-mechanism differs from those developed in other studies. Our design made use of adjustable linkages and a base platform to adjust the working space and resolution, and elastic wire joints replaced the ball joints to eliminate the six additional rotational freedoms and avoid singularity errors. Then, we presented the synthesis for the parallel micro-mechanism structure and described the control strategy. We evaluated the precision parallel micro-mechanism using a series of tests. The experimental results indicated that the developed parallel micro-mechanism could be used to manipulate micro-objects at high speed and with a high degree of precision.

In future studies, we plan to measure the working space and resolution of the parallel micro-mechanism for different parameters to fully evaluate its performance.

Acknowledgment

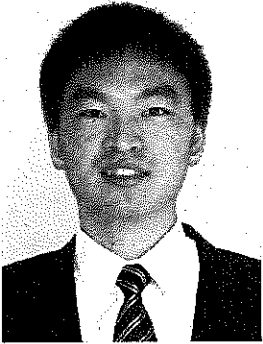
This research was supported by Kagawa University Specially Promoted Research Fund 2007 and Kagawa University Project Research Fund 2006.

References

- [1] A. Hara & K. Sugimoto, Synthesis of parallel micromanipulators, *Journal of Mechanisms, Transmission, and Automation in Design*, 111, 1989, 35–39.
- [2] F. Arai, M. Ogawa, T. Fukuda, K. Horio, T. Sone, K. Itoigawa, & A. Maeda, High speed random separation of microobject in microchip by laser manipulator and dielectrophoresis, *Proc. IEEE 13th Annual Int. Conf. on Micro Electro Mechanical Systems*, Miyazaki, Japan, 2000, 727–732.
- [3] G. Fedder, S. Santhanam, M.L. Reed, S. Eagle, D.F. Guillou, M. Lu, & L.R. Carley, Laminated high-aspect-ratio microstructures in a conventional CMOS process, *Proc. IEEE Micro Electro Mechanical Systems Workshop*, San Diego, CA, 1996, 13–18.
- [4] A. Sulzmann, J. Carrier, & J. Jacot, Virtual reality and high accurate vision feedback as key information for micro robot telemanipulation, *SPIE Proc. Microrobotics: Components and Applications*, 2906, Boston, 1996, 38–57.
- [5] A. Kawaji, F. Arai, & T. Fukuda, Calibration for contact type micromanipulation, *Proc. 1999 IEEE/RSJ Int. Conf. on Intelligent Robots and Systems*, Seoul, 1999, 715–720.
- [6] J. Wang & S. Guo, A human scale tele-operating system for microoperation: Macro/micro complex mechanism for HSTOS, *Proc. 2005 IEEE Int. Conf. on Robotics and Biomimetics*, Hong Kong and Macau, 2005, 681–686.
- [7] F. Arai, T. Sugiyama, P. Luangjarmekorn, A. Kawaji, T. Fukuda, K. Itoigawa, & A. Maeda, 3D viewpoint selection and bilateral control for bio-micromanipulation, *Proc. 2000 IEEE Int. Conf. on Robotics and Automation*, San Francisco, 2000, 947–952.
- [8] I. Pappas & A. Codourey, Visual control of a microrobot operating under a microscope, *Proc. 1996 IEEE/RSJ Int. Conf. on Intelligent Robotics and System*, Osaka, Japan, 1996, 993–1000.
- [9] L.W. Tsai, *Robot analysis: The mechanics of serial and parallel manipulators* (New York: John Wiley, 1999).
- [10] E.L. Faulring, J.E. Colgate, & M.A. Peshkin, A high performance 6-DOF haptic robot, *Proc. IEEE Int. Conf. on Robotics and Automation*, New Orleans, LA, 2004, 1980–1985.
- [11] T. Tanikawa & T. Arai, Development of a micro-manipulation system having a two-fingered micro-hand, *IEEE Trans. on Robotics & Automation*, 15(1), 1999, 152–162.
- [12] B. Dasgupta & T.S. Mruthyunjaya, A Newton-Euler formulation for the inverse dynamics of the Stewart Platform manipulator, *Mechanism and Machine Theory*, 33(8), 1998, 1135–1152.

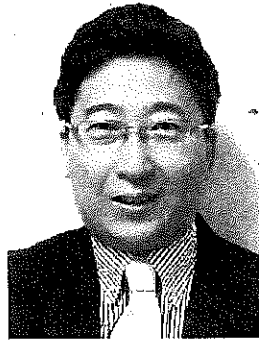
- [13] F. Pierrot, M. Uchiyama, P. Dauchez, & A. Fournier, A new design of a 6-DOF parallel robot, *Journal of Robotics and Mechatronics*, 2(4), 1990, 308-315.
- [14] B. Zhang, *Design and implementation of a 6-DOF parallel manipulator with passive force control*, doctoral diss., University of Florida, Gainesville, 2005.
- [15] D. Stewart, A platform with six degrees of freedom, *Proc. IMechE*, 180, Pt. 1(15), 1965-66, 371-385.

Biographies



Jian Wang received his B.Sc. from Changchun Institute of Optics and Fine Mechanics, Changchun, China, in 2001, and his M.Sc. from Kagawa University, Takamatsu, Japan, in 2005. Currently, he is a Ph.D. candidate at Kagawa University, Japan. His research focus is human-scale teleoperating system for biomedical applications. He has published about 10 refereed journal and

conference papers in the past three years. His interests include microrobotics and mechatronics for minimal invasive surgery. He is an IEEE student member and a student member of the Robotics Society of Japan (RSJ).



Shuxiang Guo received his Ph.D. in mechano-informatics and systems from Nagoya University, Nagoya, Japan, in 1995. Currently, he is a professor with the Department of Intelligent Mechanical System Engineering at Kagawa University. He has published about 140 refereed journal and conference papers. His current research interests include

micro robotics system for minimal invasive surgery, micro catheter system, micro pump, and smart material (SMA, ICPF) based on actuators. He has received research awards from the Tokai Section of the Japan Society of Mechanical Engineers (JSME) and the Tokai Science and Technology Foundation, and was granted the Best Paper Award of the IS International Conference, Best Paper Award of the 2003 International Conference on Control Science and Technology, and Best Conference Paper Award of IEEE ROBIO2004, in 1997, 1998, 2000, 2003, and 2004, respectively.